Chemical Engineering Journal 164 (2010) 383–392

Contents lists available at ScienceDirect

Chemical Engineering Journal

journal homepage: www.elsevier.com/locate/cej

Modelling of pharmaceutical granule size reduction in a conical screen mill

Gavin K. Reynolds

Pharmaceutical and Analytical Research and Development, AstraZeneca, Macclesfield SK10 2NA, UK

ARTICLE INFO

Article history:
Received 23 June 2009
Accepted 19 March 2010

Keywords:
Impact milling
Comil
Population balance model
Agglomerate
Breakage

ABSTRACT

Conical screen mills, such as the Comil, are ubiquitous in the secondary manufacture of solid oral dosage forms in the pharmaceutical industry. These mills are used for purposes ranging from coarse delumping to fine control of granule size. Control of granule size is important, in particular with respect to manufacturability (flow) and product quality (weight uniformity, dissolution). Population balance models are ideally suited to mechanistically modelling the change in the granule size distribution as the result of granule breakage. Use of a population balance model for granule breakage requires identifying a suitable breakage rate constant and a breakage function (or fragment distribution). A method is presented whereby assuming limited hold-up time in the mill a classification kernel can be used to model the size reduction process. This classification kernel essentially makes the population balance equation insensitive to the breakage rate, leaving only the fragment distribution to be determined. A general purpose fragment distribution is proposed that captures both the localised disintegration and multiple fragmentation modes of agglomerate impact breakage. The model accurately describes the milled granule size distribution. Additionally, the model exhibits characteristic features of dry granule size reduction in a conical screen mill, including the size reduction paradox, whereby coarser input material results in increased generation of fines.

1. Introduction

Conical screening mills, such as the Comil (Quadro, Inc.), are ubiquitous in the secondary manufacture of solid oral dosage forms in the pharmaceutical industry. These mills are used for purposes ranging from coarse delumping of wet granules to fine control of granule size. The granule size distribution is an important intermediate product attribute. For example, the granule size distribution can have a significant effect on uniformity of powder flow, and ultimately tablet weight uniformity [1]. Additionally, control of the granule size distribution is important to minimise segregation potential during compression. Furthermore, granule size, in particular the proportion of fines can often be empirically linked with tablet hardness and strength, although no universal relationship has yet been found [2]. Therefore, control of the granule size distribution is important for subsequent product quality.

The key components for a typical conical screening mill are the screen and impeller. As granules are fed into the mill, they are impacted by the rotating impeller and forced against the screen. Once the granules are sufficiently size reduced, they are able to pass through the screen and leave the mill. The impeller is typically operated with a variable speed motor, allowing a range of tip speeds to be achieved. A spacer can be used to adjust the distance between the impeller and the screen. Further refinements to this basic configuration can also be adopted [3]. The shape of the impeller arms can be changed, with circular and square cross-sectional shapes being the most common. Additionally a variety of screens can be used with variation in size, shape and profile of the apertures.

Motzi and Anderson [4] investigated the influence of screen size, impeller speed and impeller shape on asprin granules. An analysis of variance on their experimental work indicated that these three variables are all significant and interact to determine the milled granule size distribution. For a fixed impeller shape, both a decrease in screen size and in increase in impeller speed lead to a decrease in mean milled granule size. Verheezen et al. [5] investigated the milling of dry granules in a conical screen mill. They quantified the extent of milling using a size reduction ratio (SRR), essentially the ratio of milled to unmilled volume median size. They found the screen size to be the dominant process parameter for size reduction, which was attributed to increased impacts with the impeller until the granules are sufficiently small to pass through the screen. More recently Schenck and Plank [6] investigated the milling of wet and dry agglomerates in a conical screen

E-mail address: gavin.reynolds@astrazeneca.com.

1385-8947/$ – see front matter © 2010 Elsevier B.V. All rights reserved.
doi:10.1016/j.cej.2010.03.041

Nomenclature

b	fragment distribution
B	beta function
B_{break}	birth term for discretised breakage equation [$m^{-3}\ s^{-1}$]
d_{95}	particle size corresponding to 95th percentile of cumulative volume distribution [m]
D_{break}	death term for discretised breakage equation [$m^{-3}\ s^{-1}$]
H	Heaviside step function
H_k	Heaviside step function used in cell-average algorithm
k_v	volumetric shape factor
l	particle size [m]
l_c	critical size for breakage kernel Eq. (2) [m]
l_{sc}	mill screen size [m]
n	number density function [m^{-6}]
N_i	number of particles in size class i [m^{-3}]
p	number of fragments
P	volume fraction
q	sharpness coefficient for Hill-Ng daughter distribution
S	breakage rate kernel [$m^{-3}\ s^{-1}$]
t	time [s]
u	particle size [m^3]
v	particle size [m^3]
$\bar{v}_{break}$	volume average size of fragments [m^3]
$v(l)$	volume based particle size density distribution [m^{-1}]
V_i	volume fraction in size class i
z	volume fraction in disintegration mode of breakage event [−]
α	proportion of screen size apparent for particles to leave mill
χ	objective function
μ	lognormal geometric mean size [m]
σ	lognormal geometric standard deviation
υ	particle size [m^3]
ζ	bimodal distribution partition coefficient

mill. They concluded that the primary mechanism governing dry granule breakage was impact attrition. In particular, they also concluded from milling experiments in the absence of a screen, that the mill screen did not play a dominant role in determining the mode of agglomerate breakage, but only the residence time in the impact zone.

In summary, previous work investigating granule size reduction in a conical screen mill has suggested that the primary mechanism for granule breakage is from impact with the impeller, with the size of the screen influencing the residence time available for granule breakage to occur. In this paper, a mechanistic model of a conical screen mill is developed. This will allow the mode of granule breakage to be investigated, and will also be a useful tool to predict the size distribution of granules as a function of mill process parameters.

2. Numerical approach

Breakage process can be described using the continuous population balance equation:

$$\frac{\partial n(\upsilon,t)}{\partial t} = \int_{\upsilon}^{\infty} b(\upsilon,u)S(u)n(u,t)du - S(\upsilon)n(\upsilon,t) \quad (1)$$

where n is the number density function, S is the selection or breakage rate kernel and b is the fragment distribution [7]. This equation can be solved numerically in a number of ways such as using matrix methods [8], moment methods [9], and discretised or sectional methods [10–12]. The difficulty in using this approach is selecting a suitable breakage rate kernel (S) and fragment distribution (b), and in particular making these choices physically relevant. There has been some progress to base these functions on material mechanical properties for continuous materials [13,14]. However, modelling of agglomerate breakage still remains challenging due to the difficulty of measuring their intrinsic mechanical properties.

Consider the operation of a typical screening mill. Material passes into the mill, which contains a rotating impeller. Within the mill, size reduction of granules occurs by impact attrition [5,6], with the movement of the impeller forcing sufficiently small material through the screen apertures. In order to build a mechanistic model of the mill, it is assumed that the material passing through the device is relatively free flowing, such that granules smaller than the screen size have an extremely low residence time. This means that once a granule is small enough to pass through the screen, it will leave the mill without any further breakage. This seems a reasonable assumption, as a screening mill is a continuous unit operation, with limited hold-up time during granule milling (otherwise the mill would overflow during routine operation). A heaviside function can be used with a size dependent selection rate kernel to describe this classification behaviour:

$$S(l) = S_0 H(l - l_c) = \begin{cases} 0 & l < l_c \\ S_0 & l > l_c \end{cases} \quad (2)$$

where l_c is a critical size, below which granules pass freely through the screen. A first approximation could be the screen aperture. However, due to the tangential movement of the granules within the mill induced by the rotating impeller, the apparent aperture is somewhat diminished and is expected to be related to the impeller speed [3]. Using the selection rate kernel defined in Eq. (2), the population balance equation in Eq. (1) can be solved to the limit $t \to \infty$, making it insensitive to the selection rate constant, S_0. Physically, this means that granules from the input size distribution continue breaking, until their fragments are smaller than the screen size, at which point they do not break anymore (as they are assumed to have left the mill).

Sectional methods are a useful approach for solution of the population balance equation, as they allow the full size distribution to be obtained. In this class of methods, the continuous size distribution, n, is approximated by a finite number of size sections. A range of algorithms is available in the literature, and a few are now discussed. The discretised approach of Hounslow et al. [10] is formulated to ensure the number (zeroth moment) and the mass (third moment) are conserved. However, this formulation also requires a geometric discretised scheme based on $\sqrt[3]{2}$. Although experimental data can be rediscretised to fit this scheme, Eq. (2) requires some refinement near l_c. This is likely to be difficult as l_c will be at the upper end of the final size distribution and therefore a geometric discretisation that can cover the full size distribution will be fairly coarse towards the upper end. Vanni presented a formulation of the discretised breakage equation that could be solved using an arbitrary discretisation scheme. This algorithm allowed solution of the breakage equation without requiring complex analytical derivations for the fragment distribution. More recently Kumar et al. [11] proposed a cell-averaged technique which can accurately conserve number and mass for an arbitrarily discretised scheme. A brief comparison between the two algorithms was made. This approach is quite accu-

rate, even for a modest level of discretisation and was chosen for the analysis presented in this paper. It is now described in more detail.

The entire size domain is divided into a finite number I of cells. The lower and upper boundaries of the ith cell are denoted by $v_{i-1/2}$ and $v_{i+1/2}$, respectively. The total number of particles in cell i is N_i:

$$N_i(t) = \int_{v_{i-1/2}}^{v_{i+1/2}} n(u,t)du \tag{3}$$

The discretised birth and death terms of the breakage equation are given as:

$$B_{\text{break},i} = \sum_{k\geq i} N_k(t) S_k \int_{v_{i-1/2}}^{p^i} b(u, v_k)du \tag{4}$$

$$D_{\text{break},i} = S_i N_i(t) \tag{5}$$

where the limit p_k^i is given by:

$$p_k^i = \begin{cases} v_i & k = i \\ v_{i+1/2} & \text{otherwise} \end{cases} \tag{6}$$

The total volume flux as a result of breakage into the cell i is given by:

$$V_{\text{break},i} = \sum_{k\geq i} N_k(t) S_k \int_{v_{i-1/2}}^{p^i} ub(u, v_k)du \tag{7}$$

The volume average of all newborn particles in cell i is given by:

$$\bar{v}_{\text{break},i} = \frac{V_{\text{break},i}}{B_{\text{break},i}} \tag{8}$$

A set of ordinary differential equations (ODEs) is obtained by substituting these terms into the cell average formulation:

$$\begin{aligned} \frac{dN_i}{dt} = {} & B_{\text{break},i-1}\lambda_i^-\left(\bar{v}_{\text{break},i-1}\right) H\left(\bar{v}_{\text{break},i-1} - v_{i-1}\right) \\ & + B_{\text{break},i}\lambda_i^-\left(\bar{v}_{\text{break},i}\right) H\left(v_i - \bar{v}_{\text{break},i}\right) \\ & + B_{\text{break},i}\lambda_i^+\left(\bar{v}_{\text{break},i}\right) H\left(\bar{v}_{\text{break},i} - v_i\right) \\ & + B_{\text{break},i+1}\lambda_i^+\left(\bar{v}_{\text{break},i+1}\right) H\left(v_{i+1} - \bar{v}_{\text{break},i+1}\right) - S_i N_i \end{aligned} \tag{9}$$

where

$$\lambda_i^{\pm}(v) = \frac{v - v_{i\pm1}}{v_i - v_{i\pm1}} \tag{10}$$

$$H_{CA}(x) = \begin{cases} 1 & x > 0 \\ 1/2 & x = 0 \\ 0 & x < 0 \end{cases} \tag{11}$$

Given an initial condition ($n(\upsilon,0)$), a breakage function (b) and a breakage rate (S), this set of ODEs can be solved for the number distribution ($n(\upsilon,t)$).

3. Experimental

Granules were manufactured from a fixed formulation of a pharmaceutical active ingredient along with a typical brittle/ductile dual-filler mixture, binder and disintegrant. The granules were produced using a typical high-shear wet granulation process train, including dry mix, high-shear granulation with water addition, coarse wet-mass delumping, and fluid bed drying. Dried granules were retrieved for characterisation using multi-point sampling direct from the fluid bed dryer bowl. The dried granules were then size reduced in a conical screen mill (Ytron Quadro Comil 194) with a 6.35 mm spacer and using range of screen sizes and impeller speeds. The screens used in the experiments had round apertures ranging from 813 to 1397 μm. The impeller tip speeds were varied from 9.1 to 15.2 m/s (which corresponded to rotation rates of 900–1500 rpm). The milled granules were then sampled for characterisation.

Unmilled granules were sized using 20 cm diameter sieves on an Inclyno (Pascall) sieve shaker. Screens with apertures of 63, 125, 250, 500, 850, 1000, 1400, 1700, 2360 and 4000 μm were used for the size analysis. The finer milled granules were sized using a QicPic (Sympatec) with a Rodos air-dispersion unit. This technique uses high-speed image analysis and was selected to provide improved resolution of the finer milled granules.

4. Results

4.1. Selection of a fragment distribution

The experimental granule size distributions measured before and after milling are shown in Fig. 1. As would be expected of a screening mill, in all cases the milled granule size distribution is smaller than the screen size. Additionally, in all cases, the milled size distribution exhibits a bimodal distribution. Subero et al. [15] studied the impact breakage of agglomerates and found that upon impact, the mode of breakage consists of localised disintegration and crack propagation leading to multiple fragmentation. Hence, the breakage of an agglomerate in a dynamic process should be expected to yield a proportion of fine material along with several large fragments, leading to a bimodal distribution.

A bimodal lognormal distribution was fitted to the milled granule size distributions in order to quantify the modal positions, using the following equation:

$$\begin{aligned} f(l) = {} & \left(\frac{\zeta}{l\sqrt{2\pi}\ln\sigma_{1,i}} \exp\left[-\left(\frac{\ln(l/\mu_{1,i})}{\sqrt{2}\ln\sigma_{1,i}} \right)^2 \right] \right. \\ & \left. + \frac{1-\zeta}{l\sqrt{2\pi}\ln\sigma_{2,i}} \exp\left[-\left(\frac{\ln(l/\mu_{2,i})}{\sqrt{2}\ln\sigma_{2,i}} \right)^2 \right] \right) \end{aligned} \tag{12}$$

Here, μ_1 and σ_1 described the geometric mean and standard deviation, respectively, of the fine mode and μ_2 and σ_2 describe the same for the coarse mode. The parameter ζ indicates the volume fraction of the fine mode. The fitted parameters are shown in Fig. 2. The geometric mean size of the small mode is very consistent, with a mean of 58 μm, whereas the coarse mode varies over a much wider range from 289 to 470 μm. The standard errors for the geometric standard deviations of each mode are considerably larger than those for the geometric means. This is partly due to the modes of the distribution not exactly conforming to the shape of a lognormal distribution. The geometric standard deviations for both the fine mode and the coarse mode exhibit a similar range of variation.

The size distribution of the initial powder blend before processing, measured using the same sizing technique as the milled

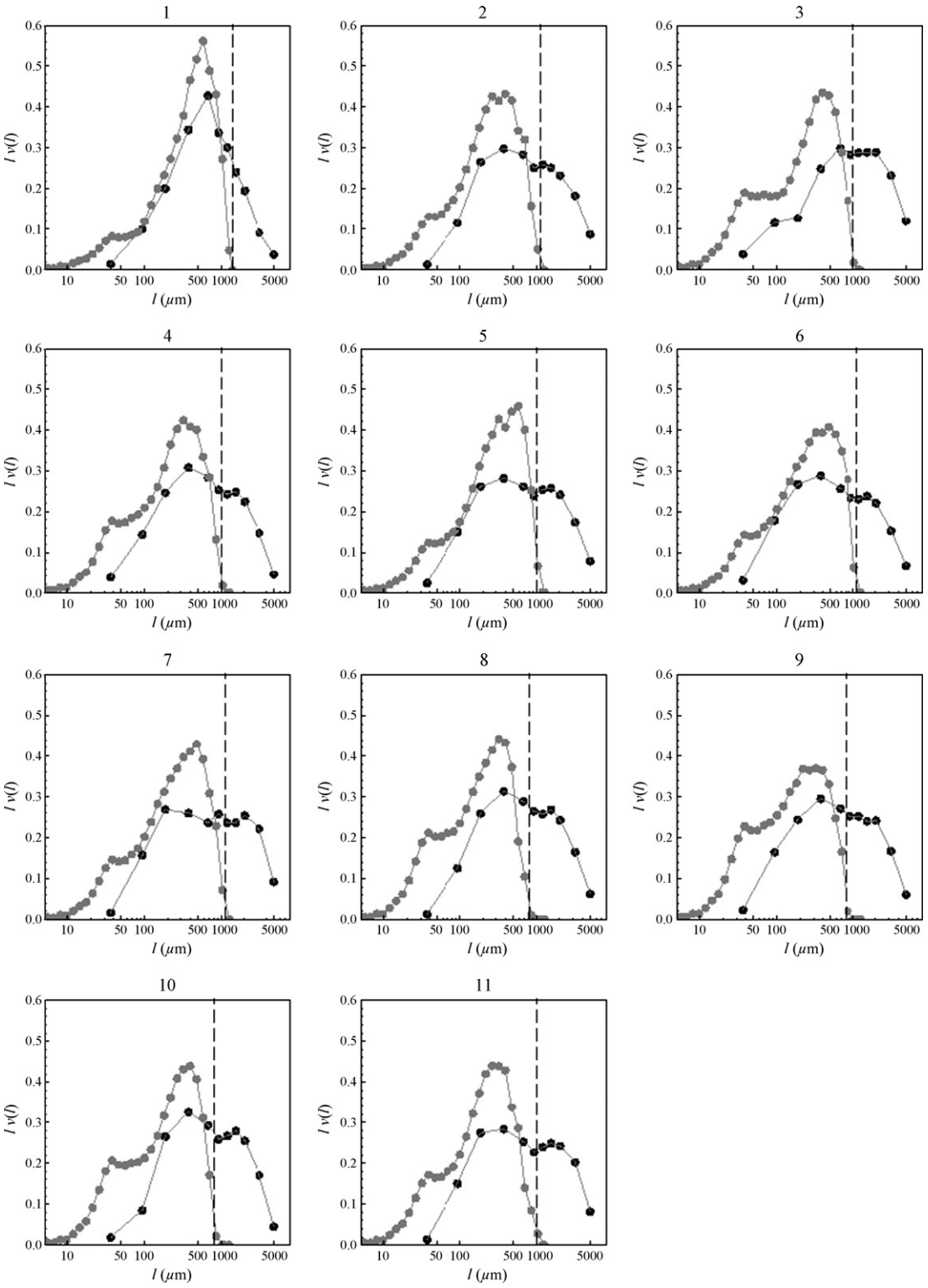

Fig. 1. Experimental granule size distributions before (black) and after (gray) milling. Vertical dashed line indicates size of screen used during dry granule milling.

granules, is shown in Fig. 3. This distribution was again parameterised by fitting to a bimodal lognormal distribution (Eq. (12)). The geometric means for each mode were determined to be 30.5 and 36.7 μm for each mode, respectively. The standard deviations were determined to be 1.4 and 2.3 for each mode, respectively. The volume fraction in the small mode was 0.4. The bimodal lognormal coefficients of the powder blend are plotted along with those for the milled granules in Fig. 2. Interestingly, the powder blend distribution is reasonably consistent with the small mode observed in the milled granule size distributions, although on average the small milled granule fragments exhibit a slightly larger and slightly broader distribution. This is reasonable, as a disintegration mechanism may not efficiently release every primary particle as a separate entity. In summary, it appears that the fine material released from the granules during milling is similar to the primary material used to create the granules (initial powder blend). Therefore the powder

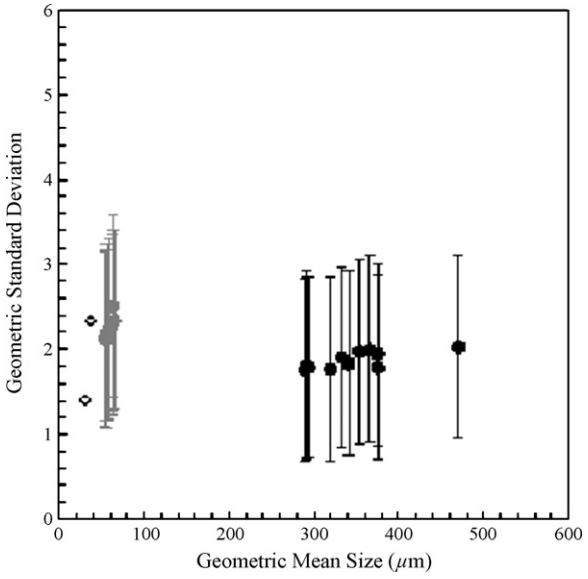

Fig. 2. Fitted bimodal lognormal coefficients for milled granule size distributions for the fine mode (gray) and the coarse mode (black). Error bars denote one standard error. Open circle symbols indicate bimodal lognormal coefficients for the raw powder blend.

blend distribution will be used to approximate the primary material release from a granule as part of a disintegration breakage mode. A suitable form for the fragment distribution, based on Hounslow et al. [10] can be expressed as:

$$b(\upsilon,u)=\frac{u}{3k_v^{1/3}\upsilon^{5/3}}\times\left[\frac{2\zeta}{\sqrt{2\pi}\,\ln\sigma_1}\frac{\exp[-(\ln(\upsilon^{1/3}/k_v^{1/3}\mu_1)/\sqrt{2}\ln\sigma_1)^2]}{1+erf[(\ln(u^{1/3}/k_v^{1/3}\mu_1)/\sqrt{2}\ln\sigma_1]}+\frac{2(1-\zeta)}{\sqrt{2\pi}\ln\sigma_2}\frac{\exp[-(\ln(\upsilon^{1/3}/k_v^{1/3}\mu_2)/\sqrt{2}\ln\sigma_2)^2]}{1+erf[(\ln(u^{1/3}/k_v^{1/3}\mu_2)/\sqrt{2}\ln\sigma_2]}\right] \quad (13)$$

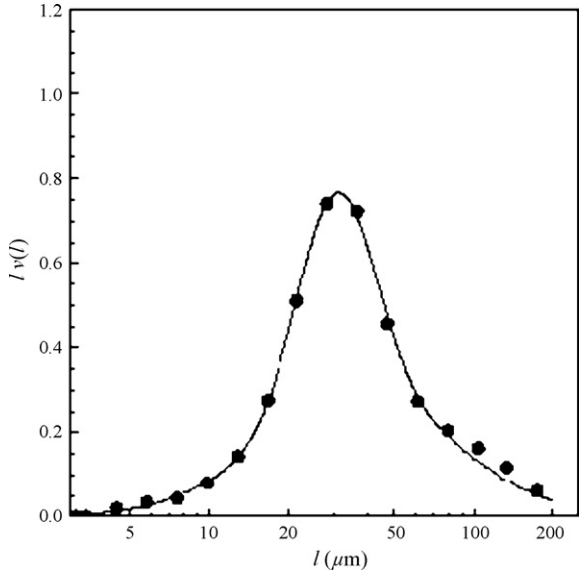

Fig. 3. Size distribution of initial powder blend. Continuous line indicates a bimodal lognormal fit.

where $k_v=\pi/6$ for a spherical particle assumption. This function assures volume conservation.

The fragmentation mode of agglomerate breakage is now considered. Diemer et al. [16] proposed a generalised form of the Hill–Ng daughter distribution, which can be expressed as:

$$b(\upsilon,u)=\frac{p}{u}\frac{(\upsilon/u)^{q-1}(1-(\upsilon/u))^{r-1}}{B(q,r)} \quad (14)$$

$$r=q(p-1) \quad (15)$$

where B refers to the beta function. The parameters p and q have fundamental meaning in this expression. The parameter p is the number of daughters (fragments) produced in a breakage event and q relates to fragment size dependence. When q is large, the distribution tends towards fragmentation. When q is small, the distribution reflects an erosion or chipping mechanism with very small fragments along with fragments near the original particle size, and little in between. Diemer et al. [16] found that there were two limiting case breakage regimes. For small values of q (erosion or chipping), the solution becomes insensitive to p (the number of fragments). For large values of q (fragmentation), the solution only depends on the number of fragments (p). They explain this as follows. In the erosion mechanism, any number of small fragments might be produced in a breakage event and this would be indistinguishable from eroding one fragment at a time, hence the independence on the number of fragments in this regime. In the fragmentation mechanism, once the distribution has formed a peak, approaching a perfect Dirac delta distribution more closely has little impact on the result, and hence the insensitivity to q in this region. The fragmentation limit of the Hill–Ng generalised daughter distribution appears to be a suitable general-purpose model to model a fragmentation process. The limiting case of this model is the uniform binary breakage function (where $p=2$).

A general purpose fragment distribution to combine both the localised disintegration and the multiple fragmentation modes of agglomerate breakage can be obtained as a volume weighted combination of Eqs. (13) and (14):

$$b(\upsilon,v)=\frac{uz}{3k_v^{1/3}\upsilon^{5/3}}\times\left[\frac{2\zeta}{\sqrt{2\pi}\,\ln\sigma_1}\frac{\exp[-(\ln(\upsilon^{1/3}/k_v^{1/3}\mu_1)/\sqrt{2}\ln\sigma_1)^2]}{1+erf[\ln(u^{1/3}/k_v^{1/3}\mu_1)/\sqrt{2}\ln\sigma_1]}+\frac{2(1-\zeta)}{\sqrt{2\pi}\ln\sigma_2}\frac{\exp\left[-(\ln(\upsilon^{1/3}/k_v^{1/3}\mu_2)/\sqrt{2}\ln\sigma_2)^2\right]}{1+erf[\ln(u^{1/3}/k_v^{1/3}\mu_2)/\sqrt{2}\ln\sigma_2]}\right]+(1-z)\frac{p}{u}\frac{(\upsilon/u)^{q-1}(1-(\upsilon/u))^{r-1}}{B(q,r)} \quad (16)$$

where z is the volume fraction of disintegrated material and $(1-z)$ is the volume fraction of large fragments.

4.2. Parameter estimation

The fragmentation function, Eq. (16), has eight adjustable parameters. As discussed, the geometric mean and standard deviations (μ and σ) of the fines and ζ will be approximated using the bimodal lognormal coefficients fitted to the powder blend distribution. Diemer et al. [16] recommend assuming $q=10$ for the fragmentation regime of the generalised Hill–Ng daughter distribution. This essentially leaves two remaining adjustable parameters,

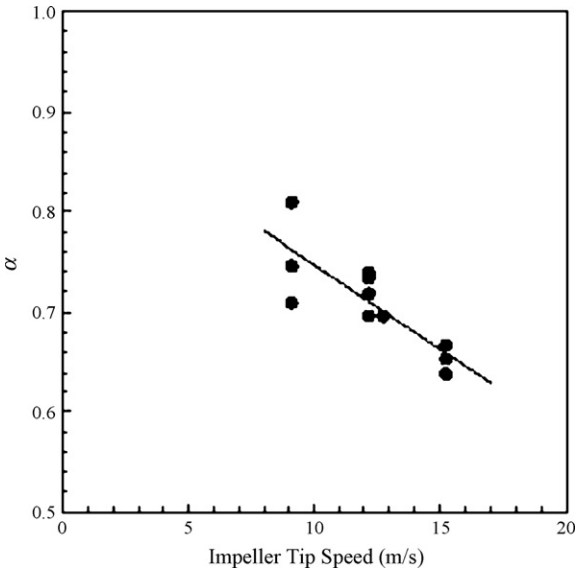

Fig. 4. Relationship between α and mill impeller tip speed. Continuous line indicates linear regression.

which are z (the volume fraction of liberated fines) and p (the number of large fragments generated from a breakage event).

Considering the selection rate kernel, Eq. (2), the critical size, l_c, can be approximated as:

$$l_c = \alpha l_{sc} \tag{17}$$

where l_{sc} is the size of the apertures in the mill screen and α is an adjustable parameter, descriptive of the reduction in apparent screen size due to the tangential movement of the particles in the mill [3]. This parameter can be considered an additional adjustable parameter to be determined simultaneously with the fragment distribution parameters. However, this parameter can also be estimated more directly by examining the maximum size of granules in each sample. The size corresponding to the 95th percentile (d_{95}) was chosen for this purpose. This choice represents a compromise between obtaining the maximum size from each sample and the uncertainty of determining the tail of the granule size distribution accurately. Therefore, α can then be estimated as:

$$\alpha = \frac{d_{95}}{l_{sc}} \tag{18}$$

where d_{95} is calculated from the milled granule size distribution. Fig. 4 shows the relationship between α and the impeller tip speed of the mill. There is a reduction in α with increasing impeller speed. This is consistent with the observation that the tangential motion of the particles within the mill can lead to a reduction in the apparent aperture of the screen due to the angle between the particles and the screen becoming more acute [3]. The relationship appears to be approximately linear within the region of impeller speeds examined. Additionally, there is some degree of scatter in the data, likely due to the difficulty in robustly determining the tail of the distribution. The linear regression coefficient was determined to be 0.68, with the following equation:

$$\alpha = 0.91 - \left(1.66 v_t \times 10^{-2}\right) \tag{19}$$

where v_t refers to the impeller tip speed.

With α estimated from Eq. (19), the total number of remaining adjustable parameters to determine was two, namely z and p in order to complete the model. This was achieved by minimizing the following objective function:

$$\chi^2(y) = \sum_i \left[P_{\text{milled},i} - P_{\text{soln},i}\right]^2 \tag{20}$$

where $y = (z,p)$, P_i refers to the volume fraction in size class i, and the subscripts milled and soln refer to the milled experimental granule size distribution and the fixed point solution of the milling population balance equation, respectively.

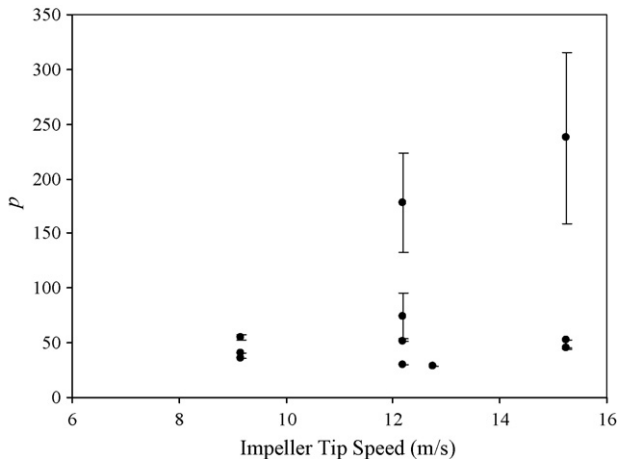

Fig. 5. Estimated fragmentation parameter p, the number of large fragments in a breakage event, plotted against impeller tip speed. Error bars denote standard error of estimate.

Fig. 5 shows the estimate of p, the number of large fragments in a breakage event, plotted against impeller tip speed. The standard error of the estimate is indicated by the error bars. There is perhaps some indication that the extent of fragmentation increases with increasing impeller tip speed. However, the key observation is that in general there is a similar level of fragmentation across the milling conditions, and with p above approximately 50 the quality of the parameter estimation deteriorates considerably.

Consider a particle of size d_0 breaking into approximately p uniform fragments. The resultant average fragment size will be

$$d_f = \frac{d_0}{p^{1/3}} \tag{21}$$

This relationship is plotted in Fig. 6, illustrating that for breakage into a few fragments, there is a large change in the resultant fragment size, but as the number of fragments increases above approximately 30, it becomes considerably less sensitive to the number of fragments. This explains the difficulty in fitting large values of p, as small changes of p in this region will only cause a very minor change in the resultant fragment distribution and hence model solution and χ^2. Due to this reason, and the consistent range of values of p for the majority batches, an average approximate value of p was selected of 40. Essentially this implies that across the range of milling conditions investigated, the fragmentation mode of breakage is relatively constant. Due to the insensitivity of the solution to large values of p, it is perhaps not correct to conclude that the fragmentation mode always consists of exactly 40 large fragments, but rather the fragmentation mode tends to include a large number of medium-sized fragments.

Based on the assumption of a constant value for p, Eq. (20) was used to fit z, but with $y = (z)$. Fig. 7 shows the estimated values of parameter z, the volume fraction in the disintegration mode of a breakage event. For the majority of screen sizes used, there is a general increase in z with increasing impeller tip speed. This seems a reasonable observation, as the increased impeller speed will result in higher impact velocities, which will result in a shift towards the disintegration mode of breakage. In the case of the smallest screen

Table 1
Summary of parameters used for model.

Parameter	Value	Units	Reason	Equation
μ_1	30.5	μm	Primary particle size distribution	Eq. (16)
σ_1	1.4	–	Primary particle size distribution	Eq. (16)
μ_2	36.7	μm	Primary particle size distribution	Eq. (16)
σ_2	2.3	–	Primary particle size distribution	Eq. (16)
ζ	0.4	–	Primary particle size distribution	Eq. (16)
q	10	–	Fragmentation limit [9]	Eq. (16)
p	40	–	Multiple fragmentation	Eq. (16)
z	$z = 0.167v_t^{0.38}$	–	Regression of estimate of z from Eq. (20) with $y = (z)$	Eq. (16)
α	$\alpha = 0.91 - \left(1.66v_t \times 10^{-2}\right)$	–	Related to largest milled granule size. Regression of Eq. (18)	Eq. (17)

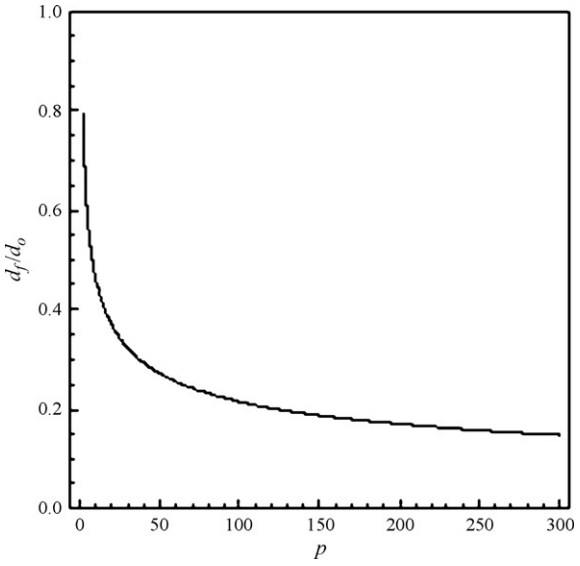

Fig. 6. Ratio of average fragment size/parent size for uniform breakage into p fragments.

size tested, 813 μm, there is a step change in z, indicating a greater generation of fines. It is possible that two of the values may be outliers, as the value of z for the highest mill speed and smallest screen aperture size is reasonably consistent with all the other batches processed with larger screen aperture sizes. There are two other possible explanations for this. Firstly, if the model is correct, and the estimated value of z does correspond to the volume fraction of material in the disintegration mode of a breakage event, then it can be concluded that the size of the screen apertures is an important factor in the breakage mode of the granules, or at least in the case of very small screen apertures. This would be inconsistent with the observation of Schenck and Plank [6] that the screen does not play a significant role in the mode of breakage. However, they did not explore the influence of such a small screen aperture size, as the smallest aperture they used was 1 mm. This same conclusion would be reached from looking at Fig. 7 in the case of screens near and above 1 mm. The second possible reason for the step change in z for the smallest screen size is a significantly increased residence time, leading to further breakage of granules that should be small enough to leave the mill. Essentially this is then a point at which the assumptions in the proposed screen mill model begin to be challenged. In particular, the assumption of the classification kernel, that as soon as granules are small enough to leave the mill they suffer no further breakage events, may not be entirely correct in the case where the mill parameters are pushed to a limit that makes it increasingly difficult for material to leave the mill, such as dramatically reduced screen aperture sizes. At this stage, it is not entirely conclusive which of these explanations is correct.

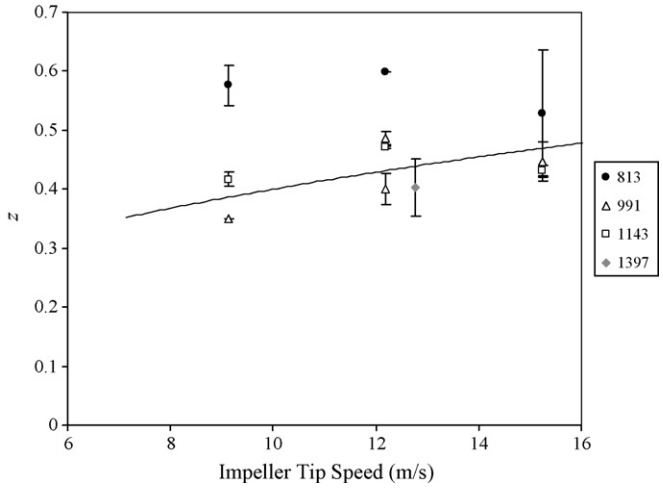

Fig. 7. Estimated parameter z, volume fraction in disintegration mode of a breakage event, plotted against impeller tip speed. Legend denotes screen aperture size in micrometres. Error bars indicate standard error of estimate. Continuous line indicates a regression power curve, with the smallest screen aperture values removed.

A power law regression curve was fitted to z as a function of impeller tip speed, with the smallest screen aperture estimates removed. This gave a relatively poor R^2 of 0.38, although the general shape of the relationship was well described by

$$z = 0.167v_t^{0.38} \tag{22}$$

With this relationship for z, milling of the granule size distributions was simulated. A summary of the parameters used in the model is provided in Table 1. A comparison of the predicted and measured milled granule size distributions is shown in Fig. 8. In general, the overall shape of the milled granule distributions are predicted very well. Batches 9 and 10, which correspond to the smallest screen aperture and low and medium impeller tip speed conditions show the largest deviation between measured and simulated. This is primarily due to the model not predicting as much fines as was measured. This is not surprising, as these batches were not used for estimating z, the proportion of the breakage mode resulting in fine material.

5. Discussion

5.1. Fragment distribution

Experimental work investigating granule size reduction in conical screen mills has concluded that the primary mechanism for granule breakage is due to impact breakage events [5,6]. Evidence from single impact experiments suggest that the mode of dry agglomerate impact breakage occurs as a combination of localised disintegration and multiple fragmentation due to crack propagation [15,17]. The fragment distribution presented in Eq. (16) is a phenomenological description of a breakage mode that includes

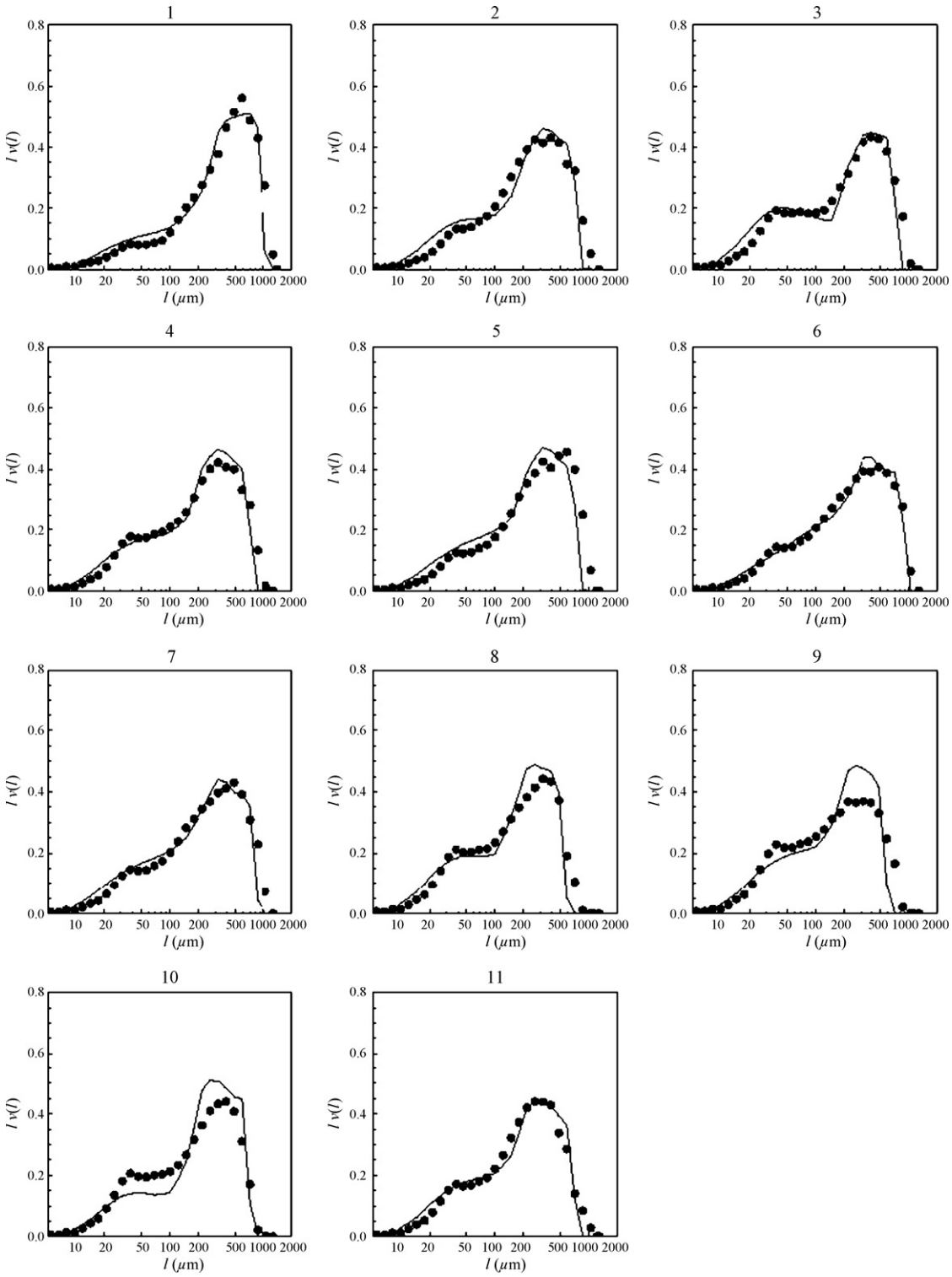

Fig. 8. Measured (points) and predicted (line) milled granule size distributions.

generation of large fragments in addition to release of fine material. Comparison of the milled granule size distributions with the primary powder distribution suggested that the fine disintegration mode of the fragment distribution could be approximated by the normalised distribution of the primary particles. There was some indication from Fig. 2 that the fine material in the milled granule size distributions was on average slightly larger than the primary material, however pragmatically using the primary particle size distribution considerably reduced the number of adjustable parameters in the fragment distribution (Eq. (16)) and still provided a good fit of the milled granule fines (Fig. 8). For other formulations, this may not necessarily the case. Material properties and indeed the structure of the granules will determine how finely divided the primary constituents of the granule become in the localised disintegration impact zone. The multiple fragmentation mode of the fragment distribution was initially estimated by fitting the experimental data. This procedure highlighted that the resultant fragment distribution rapidly becomes insensitive to the number of

fragments produced as this number is increased. A value of 40 fragments was selected to essentially indicate multiple fragmentation into 'lots of fragments'. Again, for other formulations and process conditions, this may not be the case. For example, fragmentation into 'a few fragments', say between 2 and 10 fragments would be likely to be distinguishable in the resultant milled granule size distribution. Lower impeller tip speeds and tougher agglomerates could move the fragmentation mode into this regime.

5.2. Classification kernel

The classification kernel used in this model, Eq. (2), provides a simplified model of the mode of operation of a conical screen mill. The critical size for the classification can be found relatively straightforwardly by considering the upper tail of the milled granule size distribution as shown in Eq. (17) and Eq. (18). It was found that the upper size of the milled granule size distribution is somewhat smaller than the screen aperture size, and appears to be inversely correlated with the mill impeller tip speed (Fig. 4). In general, the classification kernel appears to provide a reasonably accurate simulation of the operation of the conical screen mill, in combination with a fragment distribution descriptive of agglomerate impact breakage. Interestingly, Verheezen et al. [5] and Schenck and Plank [6] observe a seeming paradox in the operation of conical screen mills. Essentially, for the same mill conditions, in order to achieve a coarser milled product, the mill needs to be fed with a finer granulate. The explanation provided for this paradox is that for a given screen aperture size, a coarser input to the mill will require more impact breakage events before the fragments become small enough to pass through the mill. As the impact breakage events tend to produce a significant quantity of fines, through the localised disintegration mode, the resultant milled granule size distribution will contain a large proportion of fines. A numerical experiment was performed to investigate the ability of this model to exhibit this type of behaviour. The experiment is similar to that performed by Schenck and Plank [6] where specific sieved size classes of granules were milled, and then the fines percentage (defined as the % of material < 90 μm) of the milled granules quantified. Input size distributions were defined as narrow (geometric standard deviation of 1.6) lognormal distributions, with varying geometric means. These input distributions were then simulated using the model parameters defined in Table 1 for a screen aperture size of 1 mm and an impeller tip speed of 12.2 m/s. The results of this numerical experiment are shown in Fig. 9. The model supports the paradox that an increasing input granule size actually can lead to an increase in milled granule fines, without appropriate adjustment of the milling parameters.

One area where the simplistic classification kernel appears to perhaps be insufficient to describe fully the operation of the mill is in the case of particularly small screen apertures. In the case of the 813 μm aperture screen there appeared to be a step increase in the expected extent of the disintegration mode of breakage (Fig. 7). It is possible that this shift could be due to an increased residence time due to the small size of the screen apertures, and hence some degree of size reduction of material that has already been reduced below the classification size. There is also the possibility that the small aperture size may be playing a more significant role in the breakage mode. However, it seems reasonable that at some limit the simplistic classification kernel will begin become inadequate to fully describe the size reduction process. At this point some consideration will need to be made as to the expected extent of hold-up, and perhaps the size dependence of the hold-up. Overall, though, the classification kernel, combined with the combined disintegration and fragmentation fragment distribution accurately describes the milling process over the majority of milling parameters investigated.

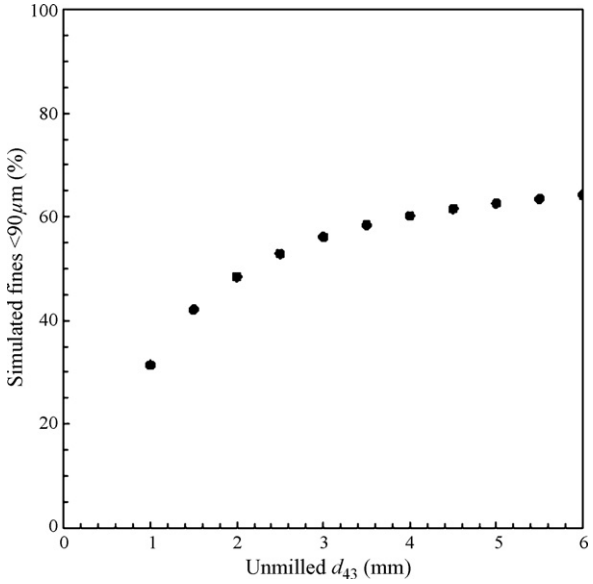

Fig. 9. Simulated milled granule fines (% <90 μm) as a function of unmilled granule size.

6. Conclusions

In this paper, a mechanistic model of a conical screen mill is presented with the following features:

- A classification kernel is used to model the mode of operation whereby only granules larger than a critical size are broken.
- A fragment distribution is proposed that captures both the localised disintegration and multiple fragmentation modes of agglomerate impact breakage.
- Accurately simulate the complete milled granule size distribution.

In general, the model output was also found to be consistent with literature observations of the size reduction of dry granules in a conical screen mill, such as:

- Impact attrition, driven by the speed of the impeller was the primary mechanism governing granule breakage.
- Size reduction paradox, whereby coarser input material leads to finer output material for constant mill operating parameters.

In summary the model offers a general purpose method to simulate size reduction in a conical screen mill. This can be of benefit for the following reasons:

- Process control. For a constant fragment distribution, which is likely to be largely determined by formulation, the model could be used for process control, such as feed-forward control of milling parameters based on the unmilled granule size distribution.
- Inferring granule mechanical robustness. Modelling of the size reduction process can be used to infer the fragment distribution, providing insight as to the mode of granule breakage. The influence of upstream material and processing changes on granule properties can be estimated if there is insufficient resource for detailed granule characterisation.

Acknowledgements

The author would like to thank Ryan Gibb, Noel Baker, Ivelisse Gonzalez and colleagues at iPR Pharmaceuticals, Inc. for their work

in producing the granule manufacturing data used in this paper. The author also thanks David Wilson for performing the milled granule size analysis.

References

[1] A.R. Fassihi, I. Kanfer, Effect of compressibility and powder flow properties on tablet weight variation, Drug Development and Industrial Pharmacy 12 (1986) 1947–1966.
[2] G. Alderborn, M. Wikberg, in: G. Alderborn, C. Nystrom (Eds.), Granule properties, Pharmaceutical Powder Compaction Technology, 2008.
[3] B. Murugesu, Milling, in: L. Augsburger (Ed.), Pharmaceutical Dosage Forms: Tablets, Vol. 1: Unit Operations and Mechanical Properties, 2008.
[4] J.J. Motzi, N.R. Anderson, The quantitative evaluation of a granulation milling process II. Effect of output screen size, mill speed and impeller shape, Drug Development and Industrial Pharmacy 10 (1984) 713–728.
[5] J.J.A.M. Verheezen, K. van der Voort Maarschalk, F. Faassen, H. Vromans, Milling of agglomerates in an impact mill, International Journal of Pharmaceutics 278 (2004) 165–172.
[6] L. Schenck, R. Plank, Impact milling of pharmaceutical agglomerates in the wet and dry states, International Journal of Pharmaceutics 348 (2008) 18–26.
[7] A.D. Randolph, M.A. Larson, Theory of Particulate Processes, Academic Press, 1988.
[8] R.H. Snow, T. Allen, B.J. Ennis, J.D. Litster, Size reduction and size enlargement, in: R.H. Perry, D.W. Green (Eds.), Perry's Chemical Engineers' Handbook, McGraw-Hill, 1997.
[9] R.B. Diemer, D.E. Spahr, J.H. Olson, R.V. Magan, S.J. Litster, Interpretation of Breakage Data via Moment Models, World Congress on Particle Technology 5, Orlando, FL, USA, 2006.
[10] M.J. Hounslow, J.M.K. Pearson, T. Instone, Tracer studies of high-shear granulation: II. Population balance modelling, AIChE Journal 47 (2001) 1984–1999.
[11] J. Kumar, M. Peglow, G. Warnecke, S. Heinrich, An efficient numerical technique for solving population balance equation involving aggregation, breakage, growth and nucleation, Powder Technology 182 (2008) 81–104.
[12] M. Vanni, Discretization procedure for the breakage equation, AIChE Journal 45 (1999) 916–919.
[13] O.M. de Vegt, H. Vromans, F. Faassen, K. van der Voort Maarschalk, Milling of organic solids in a jet mill. Part 1: determination of the selection function and related mechanical material properties, Particle & Particle Systems Characterization 22 (2005) 133–140.
[14] L. Vogel, W. Peukert, From single particle impact behaviour to modelling of impact mills, Chemical Engineering Science 60 (2005) 5164–5176.
[15] J. Subero, M. Ghadiri, Breakage patterns of agglomerates, Powder Technology 120 (2001) 232–243.
[16] R.B. Diemer, D.E. Spahr, J.H. Olson, R.V. Magan, Interpretation of size reduction data via moment models, Powder Technology 156 (2005) 83–94.
[17] G.K. Reynolds, J.S. Fu, Y.S. Cheong, A.D. Salman, M.J. Hounslow, Breakage in granulation: a review, Chemical Engineering Science 60 (2005) 3969–3992.